Dyes and Pigments 114 (2015) 129–137

Contents lists available at ScienceDirect

Dyes and Pigments

journal homepage: www.elsevier.com/locate/dyepig

Performance of zinc chlorophyll based molecules for dye sensitized solar cell

Sule Erten-Ela [a, *], Kasim Ocakoglu [b, c], Anna Tarnowska [d], Olena Vakuliuk [d], Daniel T. Gryko [d]

[a] Solar Energy Institute, Ege University, Bornova, 35100 Izmir, Turkey
[b] Advanced Technology Research & Application Center, Mersin University, Ciftlikkoy Campus, TR-33343 Yenisehir, Mersin, Turkey
[c] Department of Energy Systems Engineering, Mersin University, Tarsus Faculty of Technology, 33480 Mersin, Turkey
[d] Warsaw University of Technology, Faculty of Chemistry, Noakowskiego 3, 00-664 Warsaw, Poland

ARTICLE INFO

Article history:
Received 2 October 2014
Received in revised form
5 November 2014
Accepted 7 November 2014
Available online 15 November 2014

Keywords:
Zinc chlorophyll
Dye sensitized solar cell
Nanocrystalline TiO_2
AM 1.5 solar irradiation
J–V
IPCE

ABSTRACT

In this study, we investigated the influence of long carbon chains in ester group of the zinc chlorophyll derivatives, zinc hexyl 3-devinyl-3-hydroxymethyl-pyropheophorbide-*a* (ZnChl-C6), zinc octadecyl 3-devinyl-3-hydroxymethyl-pyropheophorbide-*a* (ZnChl-C18), zinc dodecyl 3-devinyl-3-hydroxymethyl-pyropheophorbide-*a* (ZnChl-C12) and zinc methyl 3-devinyl-3-methylhydroxymethylpyropheophorbide-*a* (ZnChl-OH), on the DSSC performance. Photovoltaic performances were determined in the order of ZnChlC12 > ZnChlC18 > ZnChlC6 > ZnChlOH from *J–V* curves. The higher J_{sc} obtained from the ZnChl-C12 sensitizer could result from the presence of long alkyl chain which reduce the charge recombination rate and facilitate electron injection. However, it was observed to decrease in the DSSC performance with the presence of longer alkyl chains (>C12). It was understood from the obtained results, the length of the alkyl chains is directly affect the DSSC performance.

1. Introduction

The research on dye sensitized solar cells (DSSCs) have quickly attracted more attention, due to their low cost production and energy conversion efficiencies compared to silicon based solar cells, after publishing the remarkable paper in 1991 by Michael Grätzel [1,2]. In dye sensitized solar cells, a dye sensitizer plays the key role in light harvesting and energy conversion [3]. Key aspects for DSSCs reside in increasing the photon collection efficiency over a broad spectrum of wavelengths in the visible regime and in retarding the charge recombination process [4–7]. The mechanism of DSSCs resembles photosynthesis. In the fascinating process of photosynthesis, water and carbon dioxide are converted into oxygen and sugar by the assistance of sunlight. In both photosynthesis and in DSSCs dyes are utilized to capture light energy. Chlorophylls are amazing compounds as a photosensitizer in visible region. They play an important role not only for light harvesting and also energy and electron transfer processes in natural photosynthesis [8–22]. Chlorophyll derivatives, which absorb at the near infrared region of solar energy have always led to high current generation and act as a driving force in developing chlorophyll sensitizers in DSSCs [22–26].

In this study, we aim to investigate the influence of long carbon chains in ester group of the zinc chlorophyll derivatives on the DSSC performance. To the best of our knowledge, there is no information regarding on this issue for zinc chlorophyll derivatives in the literature up to now.

2. Experimental section

All materials were reagent grade and were used as received unless otherwise noted.

2.1. Materials characterization

The UV–Vis absorption spectra of synthesized dyes were recorded in a 1 cm path length quartz cell by using Analytic JENA S 600. ^{1}H NMR spectra were measured on a Bruker 400 MHz spectrometer. The mass spectra were obtained via electrospray ionization (ESI-MS), and matrix-assisted laser desorption/ionization

* Corresponding author. Tel.: +90 232 3111231; fax: +90 232 3886027.
E-mail addresses: suleerten@yahoo.com, sule.erten@ege.edu.tr (S. Erten-Ela), kasimocakoglu@gmail.com (K. Ocakoglu), danieltgryko@gmail.com (D.T. Gryko).

http://dx.doi.org/10.1016/j.dyepig.2014.11.008
0143-7208/

(MALDI). Cyclic voltammetry measurements of synthesized dye were taken by using CH-Instrument 660 B Model Potentiostat equipment. Dye sensitized solar cells were characterized by current–voltage (*J–V*) measurement. All current–voltage (*J–V*) were done under 100 mW/cm^2 light intensity and AM 1.5 conditions. 450 W Xenon light source (Oriel) was used to give an irradiance of various intensities. *J–V* data collection was made by using Keithley 2400 Source-Meter and LabView data acquisition software.

2.2. Synthesis and chemical characterization of zinc chlorophyll-a derivatives

Anhydrous solvents were either distilled from appropriate drying agents or purchased from Merck and degassed prior to use by purging with dry argon and kept over molecular sieves. All chemicals were purchased from commercial sources, and used as received. Synthetic details and characterization of the compounds are described below. Molecular structures of the complexes were shown in Fig. 1.

2.2.1. Synthesis of zinc hexyl 3-devinyl-3-hydroxymethyl-pyropheophorbide-a (ZnChl-C6)

ZnChl-C6 was synthesized according to the procedures reported in the literature [27,9]. UV–VIS (MeOH) λ_{max} 652 (0.835), 605 (0.154), 575 (0.080), 528 (0.028), 426 (0.920), 407 (0.721), 324 (0.320). ^{1}H NMR (DMSO) 9.58, 9.34, 8.46 (each 1H, s, 5, 10, 20-H), 5.61 (2H, d, J = 5 Hz, 3-CH_2), 5.54 (1H, t, J = 5.5 Hz, 3^1-OH), 5.09, 5.01 (each 1H, d, J = 19.5 Hz, 13^1-CH_2), 4.54–4.48 (1H, m, 18-H), 4.27 (1H, m, 17-H), 3.95–3.90, 3.87–3.83 (each 1H, m, 17^2-$COOCH_2$), 3.76 (2H, q, J = 7 Hz, 8-CH_2), 3.58 (3H, s, 12-CH_3), 3.26 (3H, s, 2-CH_3), 3.24 (3H, s, 7-CH_3), 2.61–2.52, 2.25–2.17 (each 2H, m, 17-CH_2CH_2), 1.74 (3H, d, J = 7.5 Hz, 18-CH_3), 1.66 (3H, t, J = 7.5 Hz, 81-CH_3), 1.19–1.15 (8H, m, 172-$COOC(CH_2)_4$), 0.79 (3H, t, J = 7 Hz, 17^2-$COOC_5CH_3$). MS (ESI) found: m/z 684.3. Calcd. for $C_{38}H_{44}N_4O_4Zn$: M$^+$, 684.3.

2.2.2. Synthesis of zinc dodecyl 3-devinyl-3-hydroxymethyl-pyropheophorbide-a (ZnChl-C12)

ZnChl-C12 was synthesized according to the procedures reported in the literature [27,9]. UV–VIS (MeOH) λ_{max} 649 (0.606), 602 (0.116), 554 (0.061), 513 (0.050), 423 (0.957), 403 (0.611), 313 (0.221). ^{1}H NMR (DMSO) 9.59, 9.36, 8.46 (each 1H, s, 5,15, 20-H), 5.62 (2H, s, 3-CH_2), 5.59 (1H, br-s, 3^1-OH) 5.11, 5.02 (each 1H, d, J = 19.5 Hz, 13^1-CH_2), 4.51 (1H, m, 18-H), 4.25 (1H, m, 17-H), 3.92, 3.84 (each 1H, m, 17^2-$COOCH_2$), 3.77 (2H, q, J = 7.5 Hz, 8-CH_2), 3.59 (3H, s, 12-CH_3), 3.27 (3H, s, 2-CH_3), 3.25 (3H, s, 7-CH_3), 2.64–2.53, 2.27–2.18, (each 2H, m, 17-CH_2CH_2), 1.75 (3H, d, J = 7.5 Hz, 18-CH_3), 1.67 (3H, t, J = 7.5 Hz, 8^1-CH_3), 1.36 (2H, m, 17^2-$COOCCH_2$), 1.22–1.04 (18H, m, 17^2-$COOC_2(CH_2)_8$), 0.80 (3H, t, J = 7 Hz, 17^2-$OOC_{10}CH_3$). MS (MALDI) found: m/z 768.4. Calcd. for $C_{44}H_{56}N_4O_4Zn$: M$^+$, 768.4.

2.2.3. Synthesis of zinc octadecyl 3-devinyl-3-hydroxymethyl-pyropheophorbide-a (ZnChl-C18)

ZnChl-C18 was synthesized according to the procedures reported in the literature [27,9]. UV–VIS (MeOH) λ_{max} 652 (0.623), 607 (0.112), 575 (0.057), 528 (0.018), 426 (0.676), 408 (0.524), 324 (0.222). ^{1}H NMR (DMSO) 9.57, 9.34, 8.45 (each 1H, s, 5, 10, 20-H), 5.61(2H, s, 3-CH_2), 5.54 (1H, br-s, 3^1-OH), 5.09, 5.00 (each 1H, d, J = 19.5 Hz, 13^1-CH_2), 4.55–4.46 (1H, m, 18-H), 4.27–4.21 (1H, m, 17-H), 3.94–3.3.88, 3.86-3.79 (each 1H, m, 17^2-$COOCH_2$), 3.75 (2H, q, J = 7 Hz, 8-CH_2), 3.57 (3H, s, 12-CH_3), 3.25 (3H, s, 2-CH_3), 3.24 (3H, s, 7-CH_3), 2.65–2.50, 2.30–2.15, (2H, 1H, m, 17-CH_2CH_2), 1.74 (3H, d, J = 7 Hz, 18-CH_3), 1.66 (3H, t, J = 7.5 Hz, 8^1-CH_3), 1.30–1.04 (32H, m, 17^2-$COOC_2(CH_2)_{16}$), 0.82 (3H, t, J = 7 Hz, 17^2-$COOC_{17}CH_3$). MS (MALDI) found: m/z 852. Calcd. for $C_{50}H_{68}N_4O_4Zn$: M$^+$, 852.

2.2.4. Synthesis of zinc methyl 3-devinyl-3-methylhydroxymethylpyropheophorbide-a (ZnChl-OH) (3^{1}R/3^{1}S = 1/1) (ZnChl-OH)

Zinc methyl 3-devinyl-3-methylhydroxymethylpyropheophorbide-*a* (ZnChl-OH) (3^{1}R/S) was synthesized according to the slightly modified procedure [22]. Methyl pyropheophorbide-a (106 mg, 0.19 mmol) was dissolved in 30% hydrogen bromide in acetic acid (40 ml) and was heated at 45 °C under argon atmosphere for 4 h. Subsequently, solution was poured into ice-water, extracted with CH_2Cl_2, twice washed with H_2O, dried over Na_2SO_4 and concentrated *in vacuo*. After evaporation residue was dissolved in MeOH (50 ml), 5 ml of $H_2SO_{4(conc)}$ was added dropwise to the solution at 0 °C and left stirring overnight at ambient temperature. Afterwards, solution was poured into ice-water, extracted with CH_2Cl_2 twice washed with H_2O, dried over Na_2SO_4 and concentrated *in vacuo*. Methyl 3-devinyl-3-methylhydroxymethylpyropheophorbide-a (3^{1}R/S) was obtained with yield 49.6 mg (54%) after purification by column chromatography (0.2% MeOH/CH_2C1_2) and recrystallization from CH_2C1_2/MeOH and was used for the next step.

Methyl 3-devinyl-3-methylhydroxymethylpyropheophorbide-a (3^{1}R/S, 49.6 mg, 87.6 μmol) was dissolved in the mixture of MeOH (3 ml) and CH_2Cl_2 (12 ml). Subsequently, $Zn(OAc)_2$ (anhydrous) (19.3, mg, 87.6 μmol) was added to the resulted solution and mixture was refluxed for 3,5 h. After reaction completion, 4% $NaHCO_{3(aq)}$ was added and stirred for additional 15 min. Reaction mixture then was washed with water, dried over Na_2SO_4 and

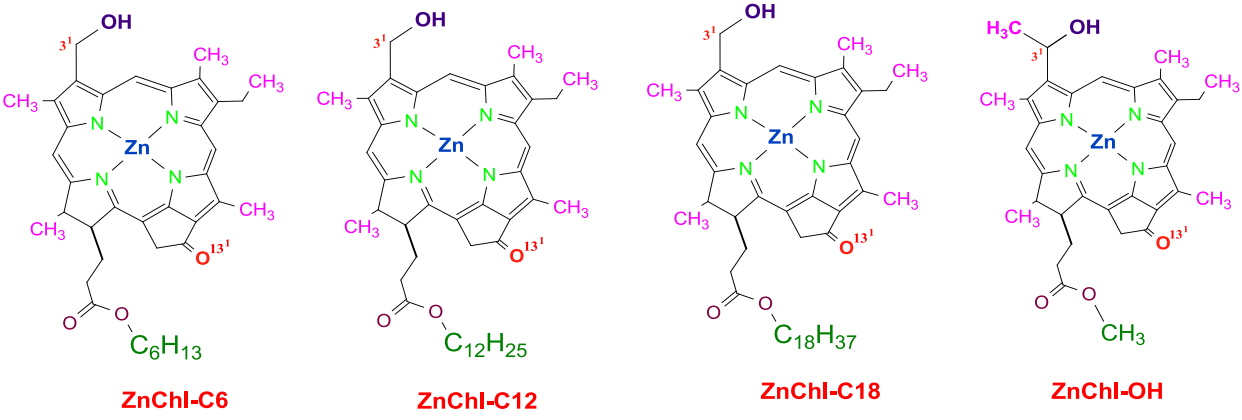

Fig. 1. Molecular structures of the zinc chlorophyll derivatives.

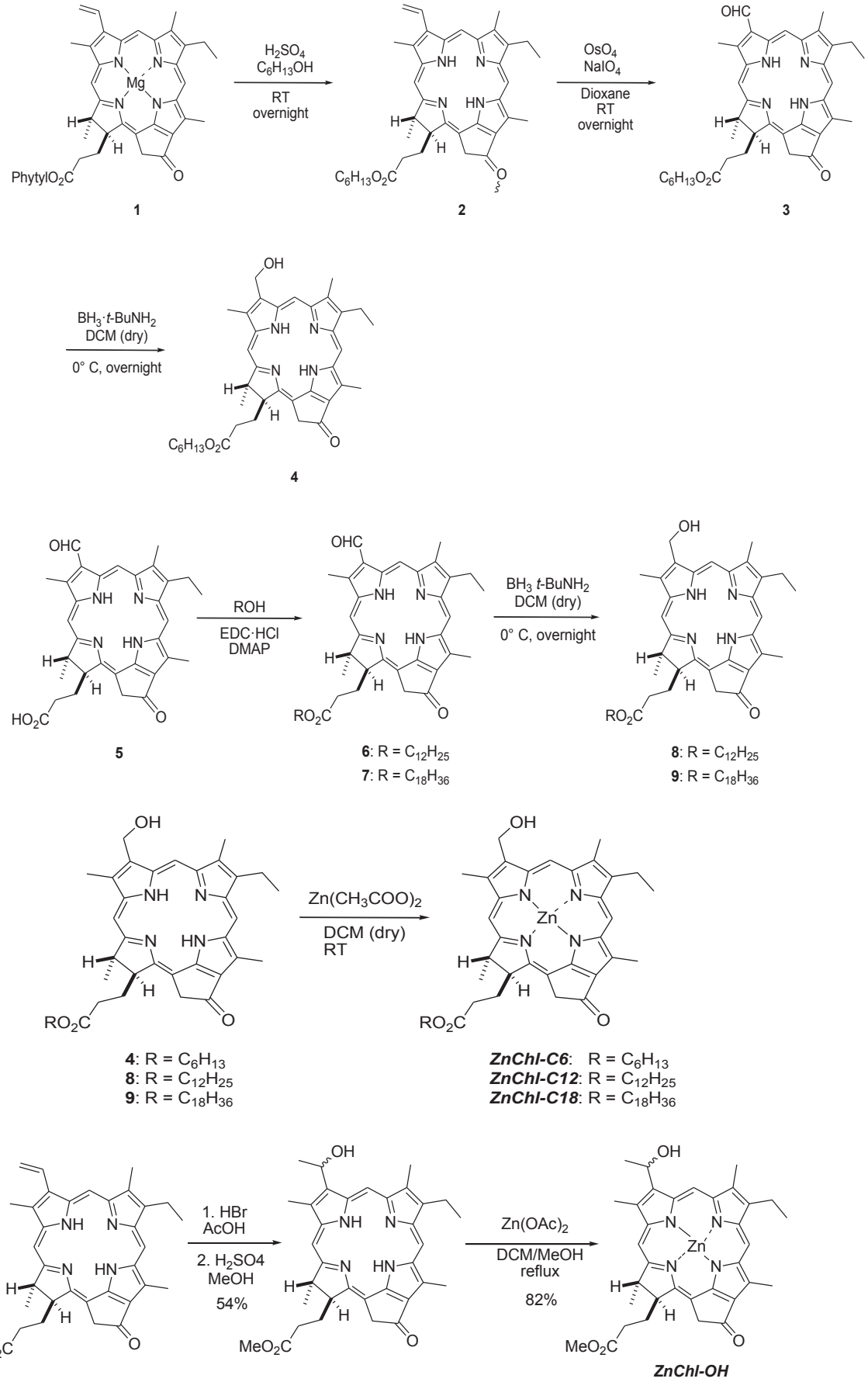

Fig. 2. Synthetic routes for the complexes, ZnChl-C6, ZnChl-C12, ZnChl-C18 and ZnChl-OH.

evaporated. The crude product was recrystalized from CH_2Cl_2/MeOH to afford corresponding zinc complex (45.1 mg, 71.9 μmol, 82%) as a dark green solid. UV–VIS (MeOH), λ_{max} 650(0.332), 602(0.063), 573(0.031), 521 (0.006), 423 (0.307), 407(0.344), 322(0.124). ^{1}H NMR (CD_3OD): 9.49, 9.39, 8.36 (each 2H, d, 5H(R/S), 10H(R/S), 20H(R/S)), 6.27 (2H, m, 3-CH(R/S)), 5.06, 4.98 (each 2H, d, J = 20 Hz, 13^1-CH_2(R/S)), 4.41 (2H, m, 18-H(R/S)), 4.14 (2H, m, 17-H(R/S)), 3.67 (4H, m, 8-CH_2(R/S)), 3.53, 3.51, 3.34, 3.21 (6H, d, 17^2-CO_2CH_3(R/S), 2-CH_3(R/S), 7-CH_3(R/S), 12-CH_3(R/S)), 2.58, 2.30(each 4H, m, 17-CH_2CH_2(R/S)), 2.08 (6H, m, 3^1-CH_3(R/S)), 1.76 (6H, d, J = 7 Hz, 18-CH_3(R/S)), 1.67 (6H, m, 8^1-CH_3(R/S)). MS (ESI) found: m/z 628; calcd. for $C_{34}H_{36}N_4O_4Zn$: M^+: 628. R_f = 0.65 (MeOH/DCM, 5:95).

Synthetic routes of chlorophyll dyes were presented in Fig. 2. And ^{1}H NMR spectra of all chlorophyll dyes were shown in Figs. 3–5.

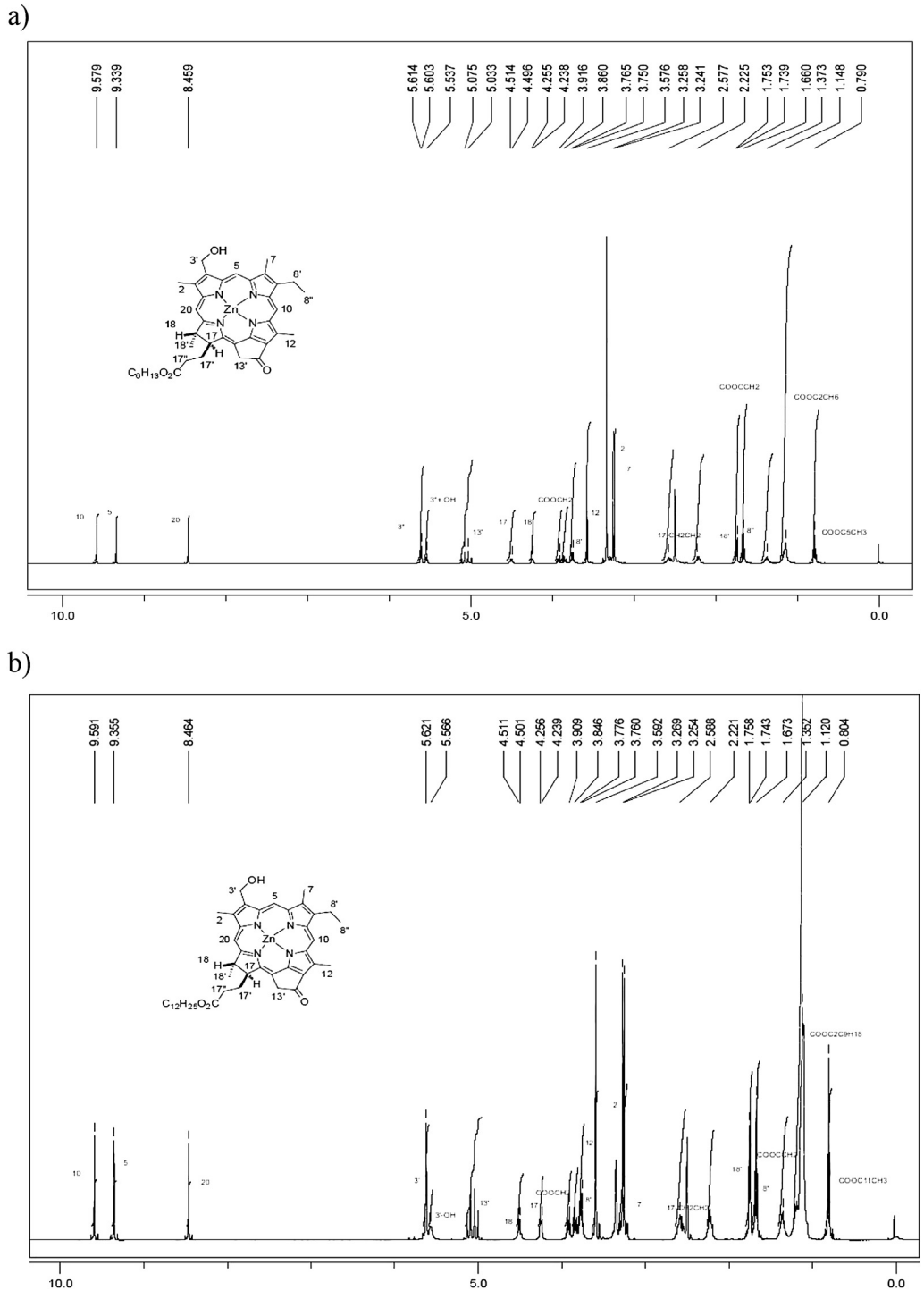

Fig. 3. ^{1}H NMR spectrum of ZnChl-C6 and ^{1}H NMR spectrum of ZnChl-C12.

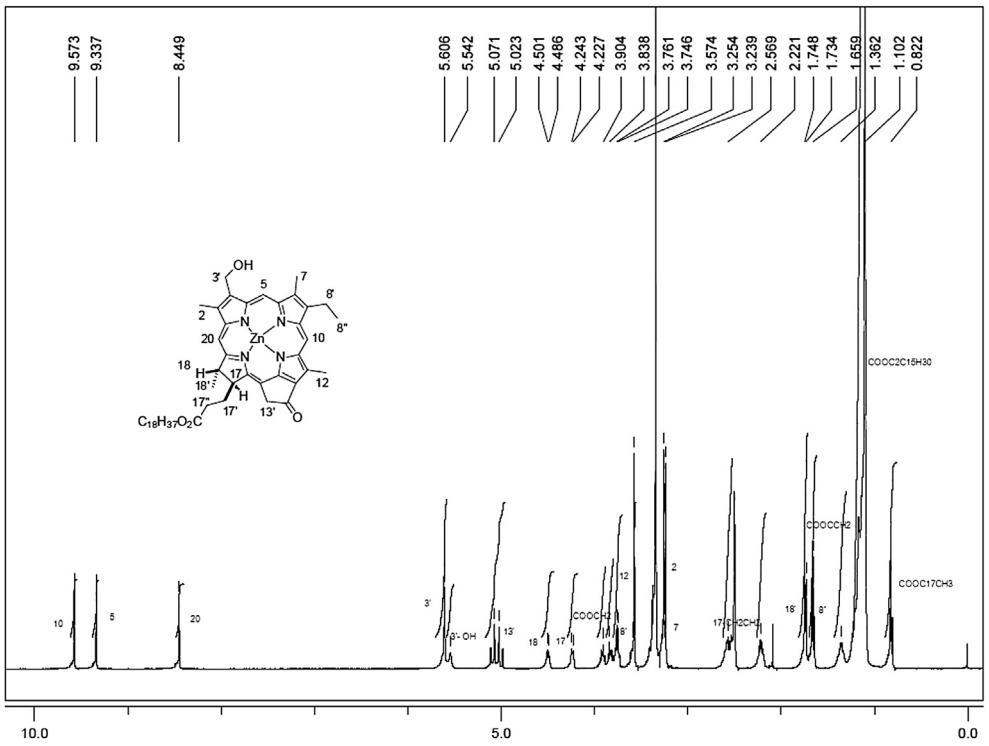

Fig. 4. ^{1}H NMR spectrum of ZnChl-C18.

2.3. Electrochemical, absorption and emission studies

The cyclic voltammograms were collected using a CH-Instrument 660 B Model electrochemical analyzer. The redox potentials of the complexes were measured using a three-electrode apparatus comprising a platinum wire counter electrode, working electrode, and an Ag/AgCl reference electrode. DMF was used as a solvent and the supporting electrolyte is tetrabutylamonium hexafluorophosphate ($TBAPF_6$), 0.1 M. Ferrocene was added to each sample solution at the end of the experiments and ferrocenium/ferrocene redox couple was used as an internal potential reference.

2.4. Photovoltaic characterization

2.4.1. Solar cell fabrication and characterization

The counter electrode consisted of FTO (TEC 8; Hartford Glass) catalyzed with platinum (Platisol, Solaronix). TiO_2 coated FTO substrates were immersed in a 0.5 mM solution of the chlorophyll complexes in acetonitrile:t-butanol:methanol (1:1:1) at room temperature overnight, and dried under a flow of nitrogen. The active solar cell area was 0.16 cm^2. The cell was sealed using a Surlyn (60 μm, Solaronix) and the 0.6 M *N*-methyl-*N*-butyl-imidazolium iodide (BMII) + 0.1 M LiI + 0.05 M I_2 + 0.5 M 4-*tert*-butylpyridine (TBP) in acetonitrile as redox electrolyte solution was introduced through pre-drilled holes in the counter electrode. The filling holes were sealed using Surlyn and a microscope cover glass.

3. Results and discussion

3.1. Synthesis

The classical protocol, utilized for the synthesis of methyl pyropheophorbide *a* was adapted to the preparation of desired hexyl derivative (**2**). It was based on oxidative cleavage of double bond, followed by reduction of the formyl group performed on the corresponding derivative (**2**) (Fig. 2) [22]. Dodecyl and octadecyl 3-devinyl-3-hydroxymethyl-pyropheophorbide *a* (**8**, **9**) were obtained from the acid derivative **5** which was prepared from Chl-*a* (**1**) via Lemieux-Jonson oxidation followed by acidic ester hydrolysis [23]. Next, the prepared product was coupled with the chosen alcohols in the presence of EDC (used for the convenience), affording dodecyl and octadecyl 3-formyl-pyropheophorbide *a* (**6**, **7**) with good yields [24]. Esters were treated with $BH_3 \cdot t\text{-}BNH_2$ to give corresponding alcohols dodecyl and octadecyl 3-devinyl-3-hydroxymethyl-pyropheophorbide *a* (**8**, **9**) (Fig. 2) [22,27]. Finally transformation of synthesized molecules into the corresponding complexes was performed via reaction of free-bases with $Zn(OAc)_2$ leading to desired compounds (**Zn-10**, **Zn-11**, **Zn-12**) (Fig. 2) [25,27]. Zinc methyl 3-devinyl-3-methylhydroxymethylpyropheophorbide-a (3^1R/S) was synthesized according to the slightly modified procedure (Fig. 2) [26].

3.2. Absorption and emission properties

The UV/Vis absorption and emission spectra of the complexes measured in THF were shown in Fig. 6, and the energy maxima and absorption coefficients were summarized in Table 1. The UV/Vis absorption spectra in Fig. 6 clearly showed that all complexes have characteristic sharp absorption peaks, which belong to the monomer form of zinc chlorophyll derivatives in the 350–680 nm region. For all samples, Soret and Q_y bands were observed at 424 and 647 nm, respectively. The high-energy and lower energy bands of the absorption spectra of the complexes was dominated by intraligand $\pi - \pi^*$ transitions. The emission spectra of the chlorophylls were obtained in an air-equilibrated THF solution at room temperature (Fig. 6). When exciting at 450 nm, all four derivatives

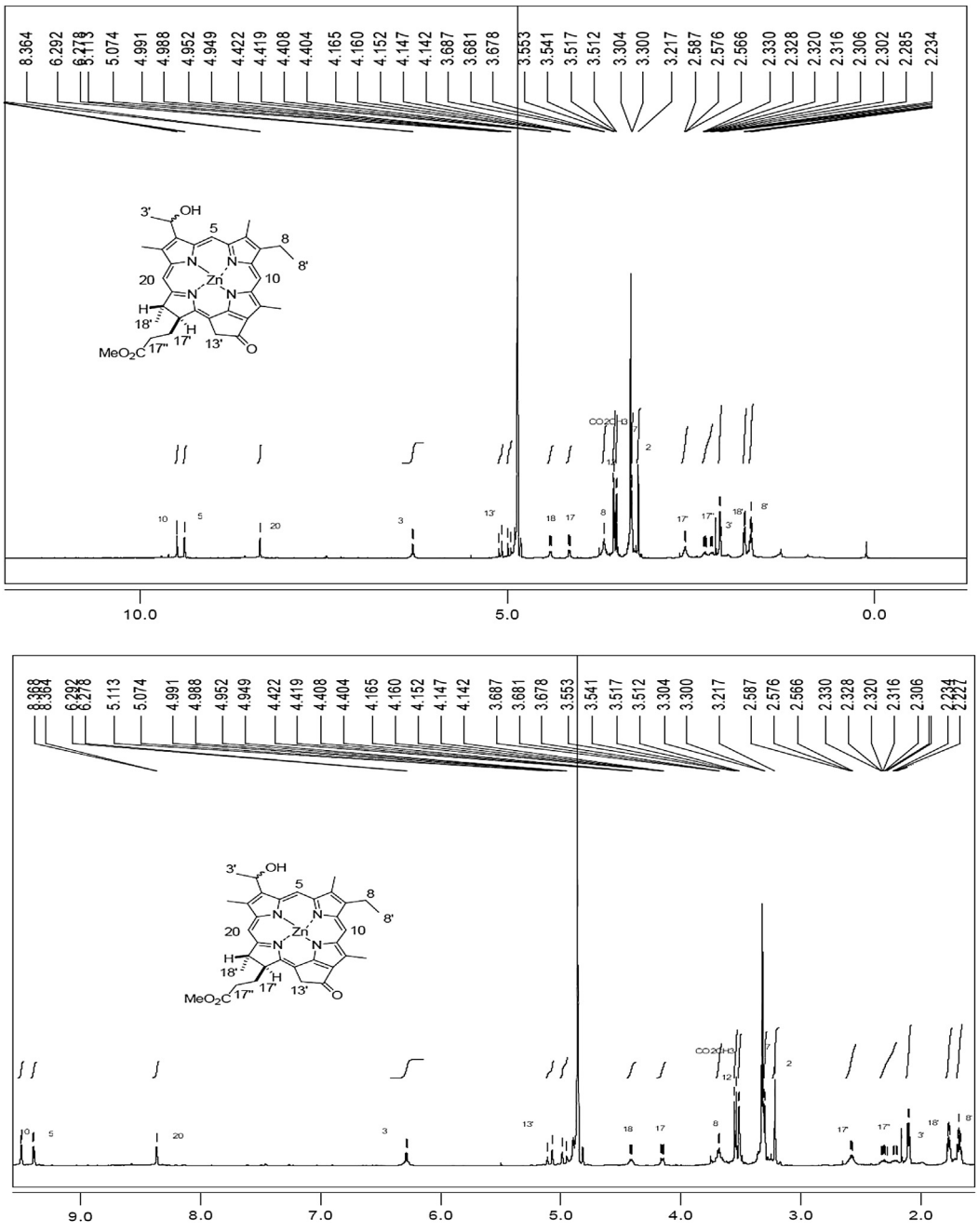

Fig. 5. ^{1}H NMR spectra of ZnChl-OH.

exhibited an intense maximum at 650 nm and a small peak at 703 nm for all samples. As expected, a small Stokes shift (3 nm) was observed due to the similar excited state and ground state geometry.

3.3. Electrochemical properties of dye

Cyclic voltammetry was employed to determine the redox potentials of chlorophyll sensitizers in Fig. 7. The electrochemical properties of the complexes have been studied in DCM. All redox potentials were calibrated *vs.* SCE. All chlorophyll sensitizers showed reversible oxidations and reversible reduction peaks. The first oxidation potentials *vs* Fc/Fc+ were listed and all results were summarized in Table 2. Their first reduction potentials corresponding to LUMO energy of the chlorophyll dyes were all higher than that of the conduction band of the TiO_2 semiconductor. Also their first oxidation potentials corresponding to HOMO energy of the chlorophyll dyes were all lower than that of I^-/I_3 redox couple. This results also ensured the generation of current in the presence of light.

3.4. Photovoltaic performance of dye sensitized solar cells

Under the solar irradiation, chlorophyll sensitizers were electronically excited which undergoes electron transfer quenching as a result of electrons being injected into the conduction band of TiO_2

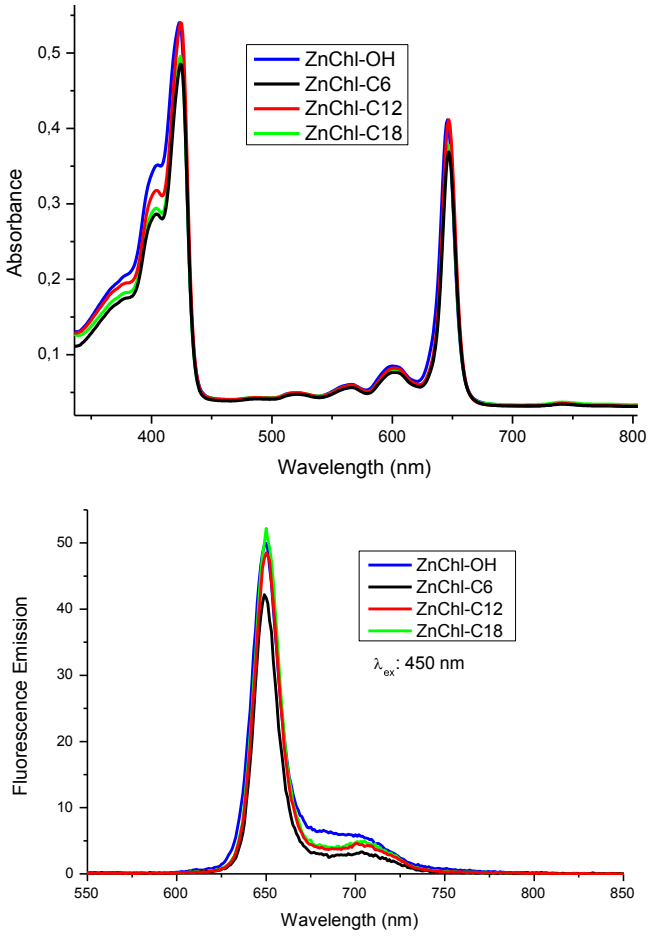

Fig. 6. UV–Vis absorption and steady-state fluorescence spectra of the complexes measured in THF. λ_{ex}: 450 nm.

semiconductor. The oxidized chlorophyll sensitizer was reduced back to the ground state by electron donor redox couple in the electrolyte. Following the general mechanism for dye sensitized solar cells, collected electrons in the conduction band pass through the external circuit to arrive at the counter electrode. The photocurrent-photovoltage and incident photon to current conversion efficiency (IPCE) of DSSCs based on chlorophyll sensitizers were presented in Fig. 8 and Table 3. Photovoltaic performances were determined in the order of ZnChlC12 > ZnChlC18 > ZnChlC6 > ZnChlOH from J-V curves. The ZnChl-C12 sensitized solar cell shows the highest performance mainly due to the high current. Indeed, the ZnChl-OH exhibit only 0.88 mA/cm^2, whereas the ZnChl-C12, shows 3.26 mA/cm^2 under the standard illumination test conditions. This higher J_{sc} could result from the presence of long alkyl chain, since it has been reported that the long alkyl chain reduce the charge recombination rate and

Table 1
UV–Vis absorption and emission properties of the complexes measured in THF. λ_{ex}: 450 nm.

Compound	λ_{max} (nm) (ε, 10^{+4} M^{-1} cm^{-1})					Emission ëmax, (nm)
ZnChl-OH	423 (5.4)	518 (0.5)	566 (0.6)	600 (0.8)	646 (4.1)	650
ZnChl-C6	424 (4.7)	520 (0.5)	566 (0.6)	601 (0.8)	647 (3.6)	650
ZnChl-C12	424 (4.9)	520 (0.5)	566 (0.6)	601 (0.8)	647 (3.8)	650
ZnChl-C18	424 (5.4)	520 (0.5)	566 (0.6)	601 (0.8)	646 (4.1)	650

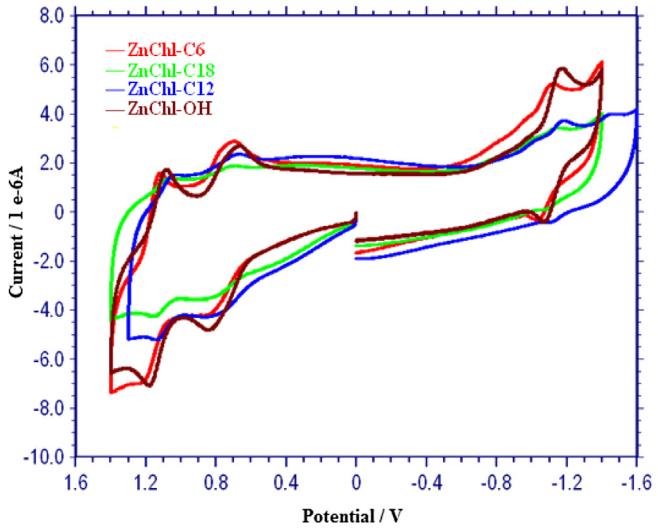

Fig. 7. Cyclic voltammogram of zinc chlorophyll derivatives.

facilitate electron injection [28]. On the other hand, the device, employing the ZnChl-C18 sensitizer, gave a lower short circuit photocurrent density (J_{sc}) of 1.65 leading to a lower power conversion efficiency while the open circuit voltage was relatively high. This lower J_{sc} may explain by poor adsorption capabilities of ZnChl-C18 sensitizer onto semiconductor surface due to their bulky structure.

4. Conclusion

The influence of long carbon chains in the ester group of the zinc chlorophyll derivatives on the DSSC performance were investigated. The results show that the length of the alkyl chains is directly affect the DSSC performance. The presence of long alkyl chains in the ester group increases the DSSC efficiency. Best efficiency was obtained with ZnChl-C12 sensitizer as 3.26 mA/cm^2 of short circuit photocurrent density, 410 mV of open circuit voltage, 0.58 of fill factor, 0.76% of overall conversion efficiency. Long alkyl chains can create a hydrophobic layer between sensitizer and electrolyte, and this causes the reduction of back electron transfer. For instance, ruthenium dyes bearing long hydrocarbon chains can act as an insulating barrier for electron–hole recombination as previously shown by Kroeze et al. [29]. Furthermore, it was also reported Kroeze et al. that ruthenium dyes with alkyl chain length from C1 to C13 dyes show closely similar injection yields, but for C18 it was observed a different situation than the others [29]. The reduced injection yield for C18 was ascribed to inhomogeneous dye loading

Table 2
Redox potentials and E_{HOMO} and E_{LUMO} levels of zinc chlorophyll derivatives.

	$E_{oxidation}$[a] (Volt)	$E_{reductio}$[b] (Volt)	$E_{ferrocene}$[c] (Volt)	E_{HOMO}[d] (eV)	E_{LUMO}[e] (eV)	$E_{Band\ Gap}$[f]
ZnChl-C6	0.77	−1.07	0.64	4.93	3.08	1.85
ZnChl-C18	0.77	−1.11	0.63	4.95	3.07	1.88
ZnChl-C12	0.76	−1.15	0.56	5.00	3.09	1.91
ZnChl-OH	0.75	−1.11	0.57	4.98	3.12	1.86

[a] First oxidation potentials of ZnChl materials.
[b] Reduction potentials of ZnChl materials.
[c] Potentials of ferrocene, internal reference electrode.
[d] HOMO energy level of ZnChl materials.
[e] LUMO energy level of ZnChl materials.
[f] Energy band gap of ZnChl materials.

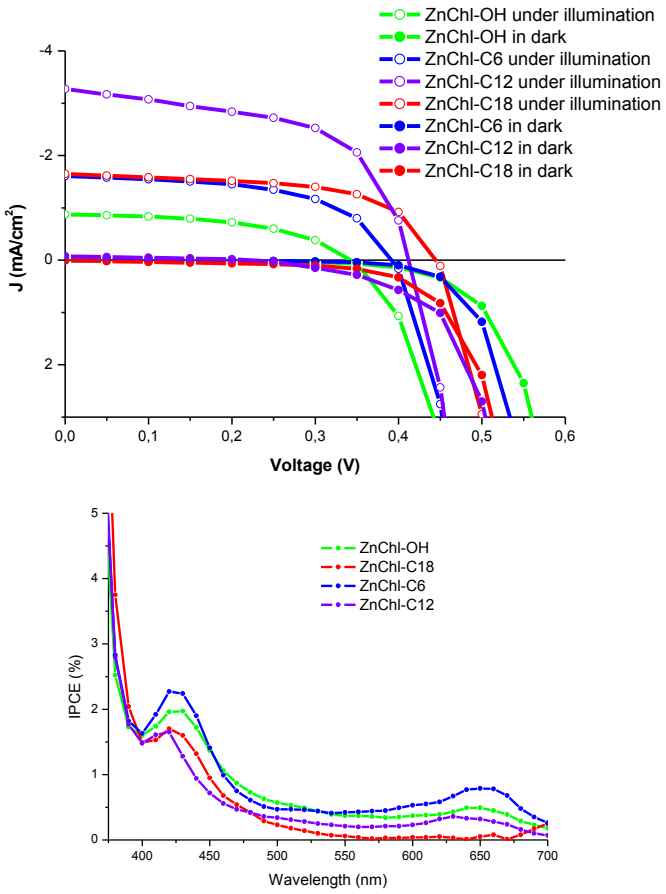

Fig. 8. *J–V* curves and incident photon to charge carrier efficiency of dye sensitized solar cells.

Table 3
Photovoltaic performance of TiO_2 based dye sensitized solar cells.

	J_{sc} (mAcm^{-2})	V_{oc} (mV)	FF	η (%)
ZnChl-OH	0.88	345	0.49	0.15
ZnChl-C12	3.26	410	0.58	0.76
ZnChl-C18	1.65	445	0.59	0.44
ZnChl-C6	1.61	395	0.55	0.35

on the TiO_2 surface due to the folding of the long C18 chains [29]. In our study, zinc chlorophyll derivatives having alkyl chains longer than twelve carbons exhibit a negative effect on the DSSC performance. This situation can be explained in a similar way. In the literature, highest efficiencies were found as 0.42% and 0.56% for ruthenium dye and polymeric metal complexes containing 8-hydroxyquinoline, respectively. Our results show better efficiency according to literature data [30–32].

Acknowledgments

We acknowledge financial support from The Scientific and Technological Research Council of Turkey (TUBITAK), Turkish Academy of Sciences (TUBA), UNESCO-Loreal Foundation and Polish National Science Center (844/N-ESF-EuroSolarFuels/10/2011/0) in the framework of European Science Foundation (ESF-EUROCORES-EuroSolarFuels-10-FP-006), and especially to Alexander von Humboldt Foundation (AvH). We thank Mechanical Engineer MSc. Cagatay Ela for illustrating of graphical abstract, proofreading and his fruithful advices.

References

[1] O'Regan B, Grätzel M. A low-cost, high-efficiency solar cell based on dye-sensitized colloidal TiO_2 films. Nature 1991;353:737–40.
[2] Grätzel M. Photoelectrochemical cells. Nature 2001;414:338–44.
[3] Wang XF, Tamiaki H. Cyclic tetrapyrrole based molecules for dye-sensitized solar cells. Energy Environ Sci 2010;3:94–106.
[4] Modesto-Lopez LB, Thimsen EJ, Collins AM, Blankenship RE, Biswas P. Electrospray-assisted characterization and deposition of chlorosomes to fabricate a biomimetic light-harvesting device. Energy Environ Sci 2010;3:216–22.
[5] Bouit PA, Marszalek M, Humphry-Baker R, Viruela R, Ortí E, Zakeeruddin SM, et al. Donor-π-acceptors containing the 10-(1,3-dithiol-2-ylidene)anthracene unit for dye-sensitized solar cells. Chem Eur J 2012;18:11621–9.
[6] Wenger S, Bouit PA, Chen Q, Teuscher J, Censo DD, Humphry-Baker R, et al. J Am Chem Soc 2010;132:5164.
[7] Ocakoglu K, Harputlu E, Guloglu P, Erten-Ela S. The photovoltaic performance of new ruthenium complexes in DSSCs based on nanorod ZnO electrode. Synth Met 2012;162:2125–33.
[8] Wang YW, Sasaki SI, Zhuang T, Tamiaki H, Zhang JP, Ikeuchi T, et al. Dicyano-functionalized chlorophyll derivatives with ambipolar characteristic for organic photovoltaics. Org Electron 2013;14:1972–9.
[9] Erten-Ela S, Tarnowska A, Vakuliuk O, Ocakoglu K, Gryko DT. Synthesis of Zinc Chlorophyll Materials for Dye-Sensitized Solar Cell Applications. Spectrochim Acta Part A;135:676–682.
[10] Pandit A, Ocakoglu K, Buda F, van Marle T, Holzwarth AR, de Groot HJM. Structure determination of a bio-inspired self-assembled light-harvesting antenna by solid-state NMR and molecular modeling. J Phys Chem B 2013;117:11292–8.
[11] Noor MM, Buraidah MH, Yusuf SNF, Careem MA, Majid SR, Arof AK. Performance of dye-sensitized solar cells with (PVDF-HFP)-KI-EC-PC electrolyte and different dye materials. Int J Photoenergy 2011;2011:960487.
[12] Tamiaki H, Shibata R, Mizoguchi T. The 17-propionate function of (Bacterio) chlorophylls: biological implication of their long esterifying chains in photosynthetic systems. Photochem Photobiol 2007;83:152–62.
[13] Kumara GRA, Kaneko S, Okuya M, Onwona-Agyeman B, Konno A, Tennakone K. Shiso leaf pigments for dye-sensitized solid-state solar cell. Solar Energy Mater Sol Cells 2006;90:1220–6.
[14] Zhang D, Yamamoto N, Yoshida T, Minoura H. Natural dye sensitized solar cells. Trans Mater Res Soc Jpn 2002;27:811–4.
[15] Wang X-F, Zhan C-H, Maoka T, Wada Y, Koyama Y. Fabrication of dye-sensitized solar cells using chlorophylls c1 and c2 and their oxidized forms c1, and c2, from Undaria pinnatifida (Wakame). Chem Phys Lett 2007;447:79–85.
[16] Amao Y, Yamada Y, Aoki KJ. Photochem Photobiol A 2004;164:47.
[17] Wanga XF, Kitaoa O, Hosonoa E, Zhoua H, Sasakic S, Tamiaki HJ. Photochem Photobiol A 2010;210:145.
[18] Tamiaki H, Xu M, Mizoguchi T. Photoreduction of zinc 3-acetyl-chlorophyll derivative to prepare chemically stable isobacteriochlorin. Tetrahedron Lett 2012;53:3210–2.
[19] Polo AS, Iha NYM. Blue sensitizers for solar cells: natural dyes from calafate and jaboticaba. Sol Energy Mater Sol Cells 2006;90:1936–44.
[20] Ikegami M, Ozeki M, Kijitori Y, Miyasaka T. Chlorin-sensitized high-efficiency photovoltaic cells that mimic spectral response of photosynthesis. Electrochemistry 2008;76:140–3.
[21] Kamat PV, Chauvet JP, Fessenden RW. J Phys Chem 1986;90:1389.
[22] Wongcharee K, Meeyoo V, Chavadej S. Dye-sensitized solar cell using natural dyes extracted from rosella and blue pea flowers. Sol Energy Mater Sol Cells 2007;91:566–71.
[23] Johnson DG, Svec WA, Wasielewski MR. Isr J Chem 1988;28:193–203.
[24] Miyatake T, Tamiaki H, Holzwarth AR, Schaffner K. Artificial light-harvesting antenna: excitation energy transfer from self-assembled zinc chlorins to a bacteriochlorin in a homogeneous hexane solution. Photochem Photobiol 1999;69:448–56.
[25] Kelley RF, Tauber MJ, Wasielewski MR. Intramolecular electron transfer through the 20-position of a chlorophyll a derivative: an unexpectedly efficient conduit for charge transport. J Am Chem Soc 2006;128:4779–91.
[26] Tamiaki H, Takeuchi S, Tsudzuki S, Miyatake T, Tanikaga R. Self-aggregation of synthetic zinc chlorins with a chiral 1-hydroxyethyl group as a model for *in vivo* epimeric bacteriochlorophyll-*c* and *d* aggregates. Tetrahedron 1998;54:6699–718.
[27] Shoji S, Hashishin T, Tamiaki H. Construction of chlorosomal rod self-aggregates in the solid state on any substrates from synthetic chlorophyll derivatives possessing an oligomethylene chain at the 17-Propionate residue. Chem Eur J 2012;18:13331.
[28] Xue X, Zhang W, Zhang N, Ju C, Peng X, Yang Y, et al. Effect of the length of the alkyl chains in porphyrin meso-substituents on the performance of dye-sensitized solar cells. RSC Adv 2014;4:8894–900.
[29] Kroeze JE, Hirata N, Koops S, Nazeeruddin Md K, Schmidt-Mende L, Gratzel M, et al. Alkyl chain barriers for kinetic optimization in dye-sensitized solar cells. J Am Chem Soc 2006;128:16376–83.

[30] Zhang L, Wen G, Xiu Q, Guo L, Deng J, Zhong C. Synthesis and photovoltaic properties of polymeric metal complexes containing 8-hydroxyquinoline as dye sensitizers for dye-sensitized solar cells. J Coord Chem 2012;65:1632–44.

[31] (a) Erten-Ela S, Sogut S, Ocakoglu K. Ocakoglu, Synthesis of novel ruthenium II phenanthroline complex and its application to TiO2 and ZnO nanoparticles on the electrode of dye sensitized solar cells. Materials Science in Semiconductor Processing 2014;23:159–66;
(b) Erten-Ela S, Ocakoglu K, Fabrication of thin film nanocrystalline TiO2 solar cells using ruthenium complexes with carboxyl and sulfonyl groups, Journal of Industrial and Engineering Chemistry, 20, 474-479;
(c) Erten-Ela S, Ocakoglu K, Iridium Dimer Complex for Dye Sensitized Solar Cells using Electrolyte Combinations with Different Ionic Liquids, Materials Science in Semiconductor Processing, 27, 532-540.

[32] Hue R, Mann KR, Gladfelter WL. Thiocyanate linkage isomerism in the isobutyl ester form of the ruthenium dye known as N3. J Coord Chem 2014;67:17–28.